Reaction Mechanisms

How to cite:
International Edition: doi.org/10.1002/anie.202218645
German Edition: doi.org/10.1002/ange.202218645

Prebiotic Synthesis and Isomerization in Interstellar Analog Ice: Glycinal, Acetamide, and Their Enol Tautomers

Joshua H. Marks, Jia Wang, N. Fabian Kleimeier, Andrew M. Turner, André K. Eckhardt, and Ralf I. Kaiser**

Abstract: Glycinal ($HCOCH_2NH_2$) and acetamide (CH_3CONH_2) are simple molecular building blocks of biomolecules in prebiotic chemistry, though their origin on early Earth and formation in interstellar media remain a mystery. These molecules are formed with their tautomers in low temperature interstellar model ices upon interaction with simulated galactic cosmic rays. Glycinal and acetamide are accessed via barrierless radical-radical reactions of vinoxy ($^{\bullet}CH_2CHO$) and acetyl ($^{\bullet}C(O)CH_3$), and then undergo keto-enol tautomerization. Exploiting tunable photoionization reflectron time-of-flight mass spectroscopy and photoionization efficiency (PIE) curves, these results demonstrate fundamental reaction pathways for the formation of complex organics through non-equilibrium ice reactions in cold molecular cloud environments. These molecules demonstrate an unconventional starting point for abiotic synthesis of organics relevant to contemporary biomolecules like polypeptides and cell membranes in deep space.

Introduction

Glycinal (**1**, $HCOCH_2NH_2$) along with its isomer acetamide (**2**, CH_3CONH_2) exemplify fundamental molecular building blocks in biochemistry and play a vital role in the structural integrity of cell walls of living organisms. Glycinal is thermodynamically less stable than **2** and rapidly undergoes condensation, making α-amino aldehydes a challenging class of compounds to study.[1] This is surprising because of the biological significance of **1**, as it is prevalently involved in the metabolism of bacteria such as the model organism Escherichia Coli.[2] In interstellar chemistry, both **1** and **2** may serve as fundamental molecular building blocks and starting materials for key biological compounds like peptides, predominantly due to their bifunctional nature. In subsequent reactions various radicals (Figure 1, **D**–**H**) may be produced by dissociation of **1** and **2** initiated by highly energetic galactic cosmic rays (GCRs). Recombination of these radicals can easily lead to interstellar prototype peptides with amide bonds, including glycine building blocks

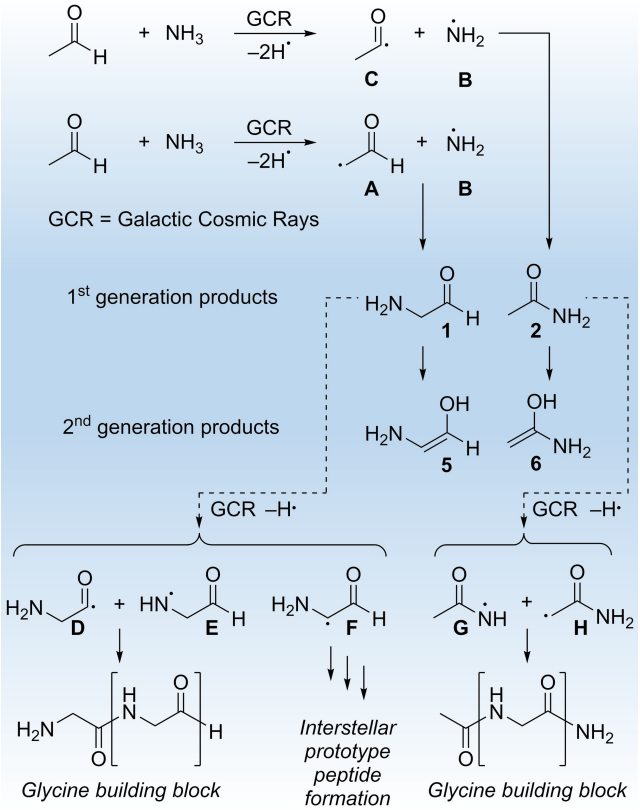

Figure 1. Preparation of **1**, **2**, and their tautomers **5**, and **6** in low-temperature interstellar ices containing acetaldehyde and ammonia through processing by GCR proxies. First-generation products **1** and **2** represent molecular building blocks for interstellar prototype peptides in radical-radical recombination reactions initiated by GCRs.

[*] J. H. Marks, J. Wang, N. F. Kleimeier, A. M. Turner, R. I. Kaiser
Department of Chemistry, University of Hawaii at Manoa
Honolulu, HI 96822 (USA)
and
W. M. Keck Research Laboratory in Astrochemistry,
University of Hawaii at Manoa
Honolulu, HI 96822 (USA)
E-mail: ralfk@hawaii.edu

A. K. Eckhardt
Lehrstuhl für Organische Chemie II, Ruhr-Universität Bochum
44801 Bochum (Germany)
E-mail: andre.eckhardt@rub.de

(Figure 1, bottom). Note that the proposed radical mechanism differs drastically from biological peptide synthesis with amino acid condensation reactions, though previous ice experiments support the possibility of this mechanism.[3]

Glycinal (**1**), by substitution of an alcohol (–OH) for the amine ($–NH_2$), is related to the simplest sugar-related compound glycolaldehyde (CH_2OHCHO), which has already been detected in space.[4] We previously demonstrated the formation of glycolaldehyde and its isomer 1,2-ethenediol (HOCHCHOH) in interstellar ice analogs, which recently led to the detection of the latter in deep space.[5] To the best of our knowledge the enol form of glycinal—2-aminoethenol (**5**, $HOCHCHNH_2$)—has not been characterized so far and is not considered in any prebiotic reaction sequences. Due to the structural analogy of **5** and 1,2-ethenediol we also expect a rapid aldol reactivity leading to sugars and amino sugars.[6] High energy tautomers of **1** and **2**, **5** and 1-aminoethenol (**6**, $H_2CC(OH)NH_2$), are likely to play a key role in the emergence of the molecules relevant to life.[7] Tautomerism is also relevant to the behavior and reactivity of amino acids and nucleic acids.[8]

The abiotic synthesis of **1** and **2** may transpire in aqueous media[9] through condensation of acetic acid with ammonia (NH_3) and in the presence of iron sulfides under hydrothermal vent conditions of elevated temperatures up to 550 K and pressures reaching 200 MPa.[10] Yet, these reactions depend on very peculiar conditions to produce thermally labile molecules, which might not have been prevalent under prebiotic conditions on early Earth.[11] An abiotic preparation of **1** and **2**, their tautomers **5** and **6**, and prototype peptides formed by reaction of **1** and **2** (Figure 1) in the interstellar medium and delivery to early Earth of these molecules and their derivatives through comets or meteorites signify a plausible source of prebiotic molecules on early Earth.[12] Amides such as **2**,[12,13] formamide ($HCONH_2$),[12] *N*-methylformamide ($HCONHCH_3$),[14] urea (NH_2CONH_2),[15] and propionamide ($C_2H_5CONH_2$)[16] have been detected in the interstellar medium in the gas phase toward the star-forming region of Sagittarius B2 (SgrB2) by rotational spectroscopy. The two simplest amides, formamide ($HCONH_2$) and **2**, were also identified on the surface of the comet 67P after the first touchdown of the Philae Lander within the framework of the *Rosetta* mission.[13a] The observation of amides in the interstellar medium support a facile formation of amides in deep space and, once incorporated into meteoritic parent bodies and delivered to early Earth, a viable origin of key molecular building blocks through an external source. At least a fraction of these abiotically synthesized compounds might be incorporated into meteoritic parent bodies and could have survived successive meteorite or comet impact on the Earth hence bolstering the hypothesis of an exogeneous delivery of key classes of prebiotic molecules to early Earth as a tempting alternative synthetic framework to hydrothermal vents. However, despite the recognized importance of **1**, **2**, **5**, and **6** in prebiotic chemistry, their abiotic formation and reaction pathways in deep space are still elusive.

Here we demonstrate the first abiotic preparation of **1** and **2** together with their tautomers **5** and **6** under experimental conditions replicating interstellar molecular cloud environments through the exposure of low temperature model ices to proxies for GCRs penetrating ices on interstellar grains in molecular clouds.[17] Within interstellar ices at 10 K, barrierless radical-radical reactions of the vinoxy (**A**, $^{\bullet}CH_2CHO$) and acetyl (**C**, $^{\bullet}C(O)CH_3$) radicals with the amino radical (**B**, $^{\bullet}NH_2$) lead to **1** and **2**, respectively, over simulated 10^6 years in molecular clouds (Figures 1 and 2); GCR-triggered tautomerization to **5** and **6**, respectively, occurs in "aged" clouds over 10^6 years mimicked in the laboratory through extended exposure of the model ices to GCR proxies (Figures 1 and 2).[18] Bodies such as the Taurus and Orion molecular clouds contain the raw material of stars and planetary systems. Interstellar dust grains—nanometer-sized carbonaceous and olivine-rich grain particles[19]—accrete ice layers of, e.g., water (H_2O), ammonia, methane (CH_4), methanol (CH_3OH), carbon dioxide (CO_2), and carbon monoxide (CO) at 10 K.[20] Complex organic molecules of astrobiological importance such as amino acids are synthesized during chemical processing by GCRs.[17b,c,21] Once a molecular cloud transitions to star-forming regions, the (organic) matter is at least partially integrated within circumstellar disks, which in turn carry the material of which planets, planetoids, and comets eventually form. Consequently, organics such as **1** and **2** plus their tautomers **5** and **6**, which are initially formed within the interstellar ices, can be incorporated into matter of Solar Systems including our own.

The simulation experiments presented here were designed to unravel the abiotic synthesis of **1** and **2** along with their tautomers **5** and **6** through the exposure of polar model ices of acetaldehyde (CH_3CHO) and ammonia to proxies of GCRs in the form of high-energy electrons mimicking conditions of the lifetime of molecular clouds of up to a few million years.[18d] These model ices were selected to demonstrate the proof-of-concept that **1** and **2** together with **5** and **6** can be formed through non-equilibrium processes within interstellar ices. The Spitzer Space Telescope surveys suggest that ices containing ammonia at levels of up to 31 % relative to water were detected toward low-mass young stellar objects.[22] Acetaldehyde has been inferred on low temperature interstellar grains at levels of a few percent with respect to water; nevertheless, laboratory experiments revealed that acetaldehyde can be produced on interstellar grains containing methane and carbon monoxide.[17b,c] In the present study, *functional groups* of synthesized organics (including **1** and **2** along with **5** and **6**) were identified via in situ infrared (IR) spectroscopy, while an explicit *isomer selective* identification of the molecules subliming during the temperature-programmed desorption phase (TPD) through heating of the exposed ices to 320 K was achieved through tunable photoionization reflectron time-of-flight mass spectrometry (PI-ReToF-MS) and isotopic substitution experiments.[23] The warm-up phase simulates the transition from a molecular cloud to a star-forming region and delivers the molecules into the gas phase, where they can be searched for by powerful radio telescopes and identified via microwave spectroscopy thus expanding our fundamental knowledge of key chemical reactions how precursors to the

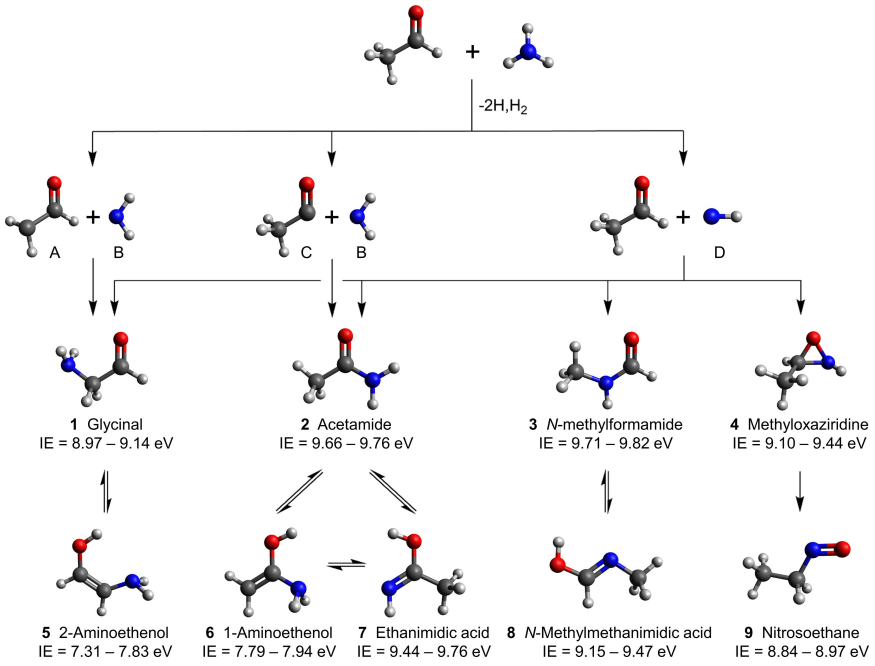

Figure 2. Reactions of radicals produced by energetic processing of acetaldehyde and ammonia. Barrierless radical-radical reactions **A** plus **B** and **C** plus **B** produce **1** and **2**, respectively. Insertion of **D** into CH or CC bonds of acetaldehyde can result in **1**, **2**, or **3**; addition of **D** to the C=O bond may form **4**. Tautomerization of these four reaction products may lead to **5**, **6**, **7**, and/or **8**.

origin of life as we know it can be synthesized in our universe.

Results and Discussion

The infrared spectra of the ices of the acetaldehyde-ammonia system were collected before, during, and after the radiation exposure (Supporting Information Table S1 and Figures S1 and S2). Radicals **A** and **C** were observed, and their observation after irradiation provides substantive evidence of the reaction scheme shown in Figure 2. With the notable exception of **A** and **C**, IR spectra of a complex mixture of organics can only assign *functional groups* of these newly formed molecules. A unique identification of reaction products is accomplished through the exploitation of PI-ReToF-MS during the TPD phase, during which the irradiated ices are warmed up to 320 K. PI-ReToF-MS affords the identification of distinct isomers in the gas phase based on their adiabatic ionization energies, threshold ionization energies, and desorption profiles as detailed below.[24] Photoionization represents an elegant tool for an ideally fragmentation-free or "soft" ionization of the target molecule thus aiding in an assignment of mass-to-charge ratios (m/z) of specific isomers.[25] The PI-ReToF-MS experiments were carried out utilizing ices of acetaldehyde and ammonia (Figure 2) along with isotopically labeled counterparts (Supporting Information Figures S3–S5) to verify the molecular formula of reaction products and to investigate the reaction mechanisms. Since the adiabatic ionization energies of **1**–**9** (Figure 2) are either unreported or were measured with errors too high to aid the PI-ReToF-MS analysis, they were computed with high confidence (Supporting Information). The average error of ± 0.05 eV and a reduction in measured ionization energies of 0.03 eV due to the ion extraction electric field of the time-of-flight spectrometer were taken into account for the design of our following experimental studies (Figure 2, Supporting Information Table S2 and Figure S6).[26]

In ices containing acetaldehyde-d_4 (CD_3CDO) and ammonia, radicals **A**-d_3 and **C**-d_3 contain three deuterium atoms. If these radicals recombine with the undeuterated **B** to produce **1** or **2**, the resulting products have the molecular formula $C_2H_2D_3NO$ ($m/z = 62$) (Supporting Information Figure S7). If (NH) was formed and then reacted via insertion, the resulting products would be **1**, **2**, **3**, and **4**; however, these insertion products would share the formula C_2HD_4NO and hence would have a distinct $m/z = 63$ compared to the radical-radical recombination products ($m/z = 62$). The PI-ReToF-MS data for the acetaldehyde-d_4 and ammonia system are shown in Figures 3a and 3b. A photon energy of **9.93** eV should ionize **1**, **2**, **3**, and **4** if present. For the low irradiation dose employed for the experiments shown in Figures 3a and 3b it is unlikely that tautomerization will occur based on prior experiments in which this reaction has been observed, and only "first-generation" reaction products are anticipated.[27] However, the order of magnitude larger doses used for the experiments shown in Figures 3c and 3d should readily initiate the sequential reactions necessary for initial carbonyl formation followed by keto-enol tautomerization.

The PI-ReToF-MS mass spectra in Figure 3 all depict ion detections at $m/z = 62$. The signal which is not observed in experiments without irradiation is the direct result of

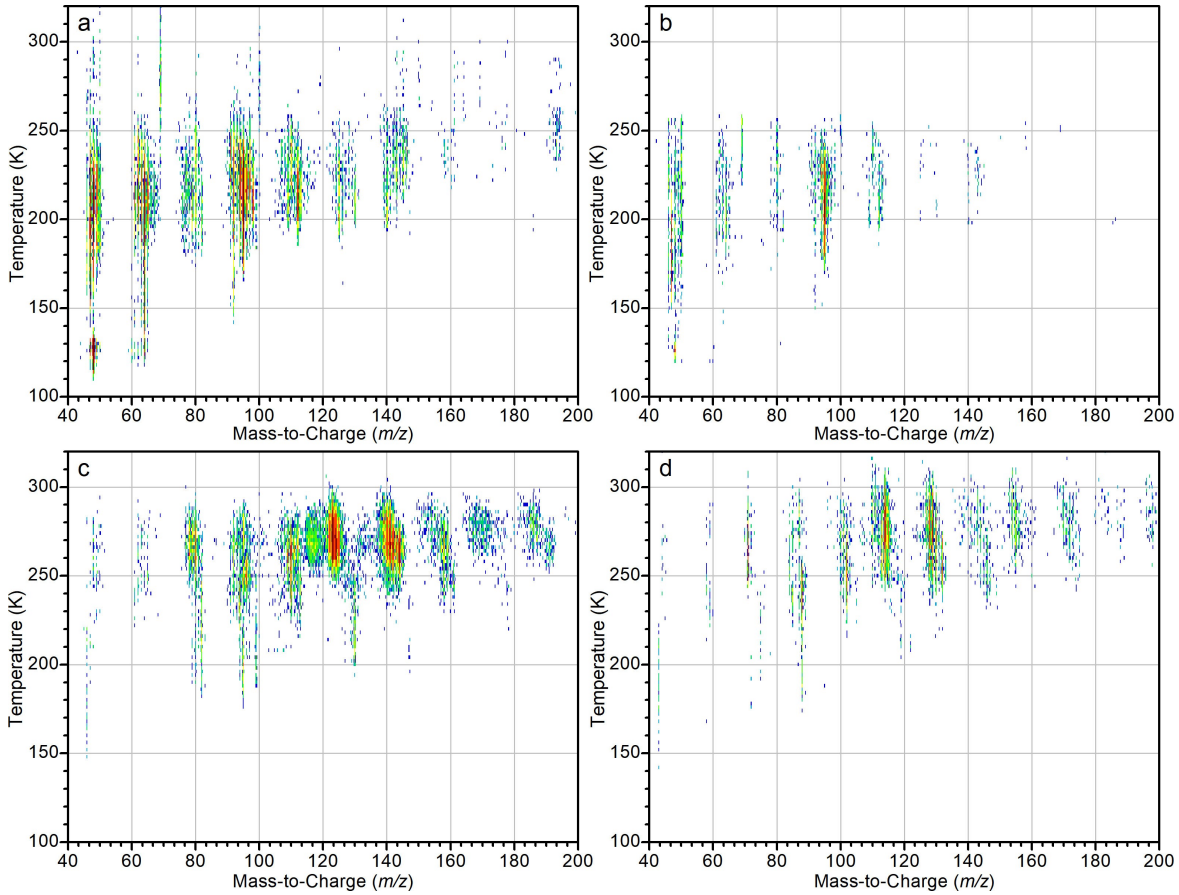

Figure 3. PI-ReToF-MS data as a function of temperature and *m/z* during the TPD of the analog ices. Data were collected for acetaldehyde-d_4-ammonia ices with a dose of 0.41 ± 0.06 eV per molecule of acetaldehyde-d_4 and 0.15 ± 0.02 eV per molecule of ammonia at 9.93 eV (a) and 9.50 eV (b) as well as for acetaldehyde-ammonia ices exposed to a dose of 3.9 ± 0.5 eV per molecule of acetaldehyde and 1.5 ± 0.2 eV per molecule of ammonia with photoionization at 8.81 eV (c) and 8.71 eV (d).

chemical reactions proceeding from irradiation. Low-intensity signal was observed for $m/z = 62$ from ices without irradiation in the range 100–200 K which has been subtracted to yield the TPD profiles observed with **9.93** eV photons (Figure 4a). Minor ion counts were observed at $m/z = 63$ as well, but at levels accounted for by naturally occurring ^{13}C and ^{15}N and sample isotopic purity. This reveals that insertion reactions of **D** are absent in the acetaldehyde-d_4 and ammonia ices. Because insertion pathways are the exclusive reaction mechanisms to **3** and **4**, these isomers must not be formed under our experimental conditions. However, ion signal was detected at $m/z = 62$ (Figure 3a); this is also evident from the corresponding TPD profile (Figure 4a), which can be linked to **1** and/or **2**. Despite the poorly resolved shoulder, the TPD profile can be deconvoluted into two discrete sublimation peaks reaching maxima at about 208 K and 237 K. A reduction of the irradiation dose results in two well-resolved sublimation events (Figure 4b). Since the relative intensities of these sublimation events changes from 8 ± 2:1 for the high dose to 1.5 ± 0.4:1 for the low dose experiment, both sublimation events must be linked to distinct isomers.

Exploiting PI-ReToF-MS, **1** and **2** can be distinguished based on their adiabatic ionization energies calculated at the CCSD(T)/CBS//B3LYP/cc-pVTZ level of theory (Supporting Information Table S2 and Figure S8). By reducing the photoionization energy from **9.93** eV to **9.50** eV, isomer **2** cannot be photoionized and signal at $m/z = 62$ must originate from **1**. The corresponding TPD profile (Figure 4c) exhibits one prominent sublimation peak reaching a maximum at about 231 K. A comparison of the TPD profiles collected at **9.93** eV (Figures 4a/b) and **9.50** eV (Figure 4c) suggests that the early sublimation event at 208 K (Figure 4a) and 203 K (Figure 4b) is linked to **2**, whereas the late event is associated with **1**. Overall, results from the acetaldehyde-d_4 and ammonia system reveal that these "first-generation products" **1** *and* **2** are both detected.

At a photon energy of **8.81** eV, "second generation products" **5** and **6** are expected to be photoionized. At a photon energy of **7.60** eV, isomer **6** cannot be ionized, and ion counts can only arise from high energy conformers of **5** (Table S2). Since tautomers are "second-generation products", experiments at photon energies of **7.60** eV and **8.81** eV were carried out with an order of magnitude higher doses to promote tautomerization of **1** and **2**. Figure 5a

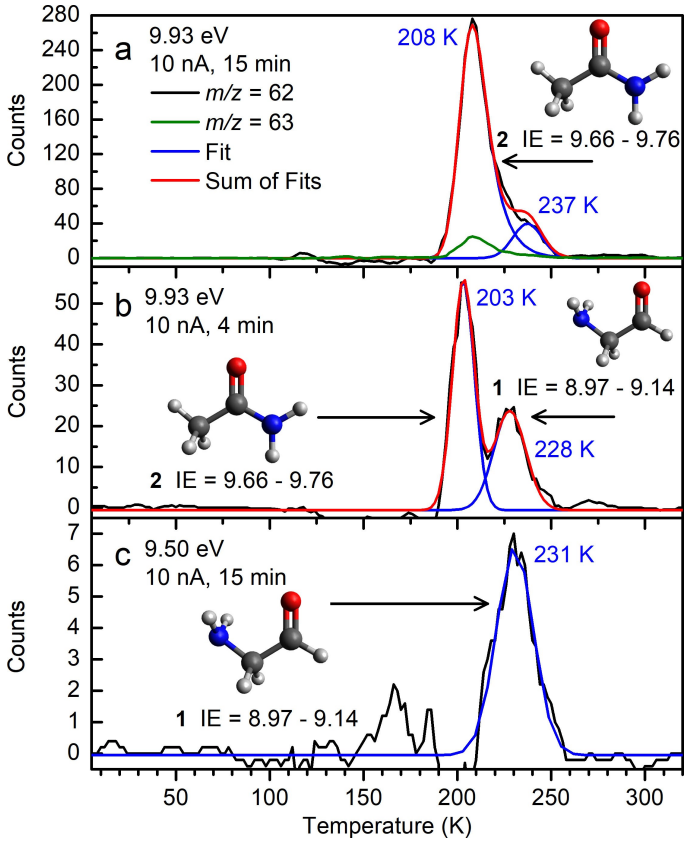

Figure 4. Ion signal of $m/z = 62$ and 63 during the TPD phase of acetaldehyde-d_4 and ammonia ice shown as a function of temperature. (a) Two convoluted peaks are observed for $m/z = 62$ at 208 K and 237 K at 9.93 eV and a dose of 0.41 ± 0.06 eV per molecule of acetaldehyde-d_4 and 0.15 ± 0.02 eV per molecule of ammonia, while no new features are observed for $m/z = 63$. (b) The relative intensity of these peaks varies with a reduced irradiation dose of 0.12 ± 0.02 eV per molecule of acetaldehyde-d_4 and 0.041 ± 0.006 eV per molecule of ammonia. (c) 9.50 eV was not found to ionize the isomer responsible for the lower temperature peak.

shows the TPD profiles of $m/z = 59$ recorded at **7.60** and **8.81** eV in acetaldehyde-ammonia ices. With a photon energy of **8.81** eV, two sublimation events were observed at peak temperatures of 227 and 270 K, while neither peak was detected at **7.60** eV. The signal at **8.81** eV reveals that **5** and/or **6** are present. A reduction of the photon energy from **8.81** to **8.71** eV, which can still photoionize both **5** and **6**, also results in two sublimation events (Figure 5a). However, the integrated peak areas of the "early" and "late" sublimation event differ strongly from $1:1.7 \pm 0.1$ at **8.81** eV to $1.6 \pm 0.1:1$ at **8.71** eV confirming that these peaks originate from two different isomers or conformers. An analysis of the conformers of **5** (Table S2) suggests that conformers **5b**–**5d** should be ionized if present. Therefore, this restricts the identity of the two observed molecules to **5a** or either of the two possible conformers of **6**, **6a** and **6b**.

Finally, to verify the molecular formulae of the observed molecules, isotopic labeling in the form of acetaldehyde-$^{13}C_2$-ammonia and acetaldehyde-d_4-ammonia ices was implemented at a photon energy of **8.81** eV (Figure 5b). This is expected to shift the masses by 2 amu and 3 amu to $m/z = 61$ and 62, respectively. The corresponding TPD profiles reveal the previously observed bimodal profiles. Detecting this bimodal pattern at $m/z = 61$ from ice containing acetaldehyde-$^{13}C_2$ confirms that the molecule observed at $m/z = 59$ contains two carbons. The TPD profile at $m/z = 62$ from ices that contain acetaldehyde-d_4 exposes the presence of at least three hydrogen atoms. This restricts the possible closed-shell molecular formula to C_2H_5NO.

The overlapping range of calculated adiabatic ionization energies of **5a** (7.73–7.83 eV) and **6a/6b** (7.84–7.94 eV for **6a**, 7.79–7.89 eV for **6b**) prevents us from concluding which of the sublimation events at 227 K and 270 K is associated with which species. PIE measurements, which report the intensity of the ion counts at $m/z = 59$ versus the photon energy, are collected to determine the onset of ionization and to permit a comparison between the experimentally measured PIE curve and ab initio simulations. This simulation requires computation of the Franck–Condon factors accounting for the differences in equilibrium geometry and vibrational structure between the neutral and radical cation under consideration (Supporting Information Table S3).[28] Franck–Condon simulations for the molecules in question predict a rapid onset of ionization at about 7.85 eV for both **5a** and **6b**, while **6a** is expected to have a gradual onset of ionization due to poor Franck–Condon factors for adiabatic photoionization. If the onset of ionization is gradual, then the PIE may be too low to detect ionization near the predicted adiabatic ionization energy; rather, efficient vertical ionization would be observed at higher energies.

A photon energy in the range of **7.73–7.92** eV was employed during TPD of irradiated acetaldehyde-ammonia ice at 216–238 K and the resulting ion yield for $m/z = 59$ are depicted in Figure 6. While both **5a** and **6b** are predicted to have similar adiabatic ionization energies, the predicted PIE curve for **5a** is in excellent agreement with experimental data. A sigmoid profile is predicted for the PIE curve of **6b** due to relatively widely spaced vibronic transitions underlying the Franck–Condon factors. This shape is not evident in these measurements and the PI-ReToF-MS signal observed in Figure 5 at 227 K is assigned to **5a**. The threshold energy for photoionization was calculated with a linear fit to the region of data in which photoionization begins which demonstrates an adiabatic ionization energy of 7.83 ± 0.01 eV.

Photon energies in the range of **7.73–8.65** eV were employed during TPD at 262–285 K to measure a PIE curve of the species subliming from irradiated acetaldehyde-ammonia ice at 270 K (Figure 6b). No photoionization is detected in the region where adiabatic ionization is expected to take place (7.84–7.94 eV), rather, ionization is found to occur with gradually increasing intensity as photon energy increases past 8.40 eV. This is nice agreement with the Franck–Condon simulation, which predicts low adiabatic ionization efficiency due to a large geometry change between the neutral and radical cationic states. The apparent increase in ionization energy is due to vertical instead of adiabatic ionization, with an apparent onset of ionization at 8.41 ± 0.03 eV due to negligible signal at lower

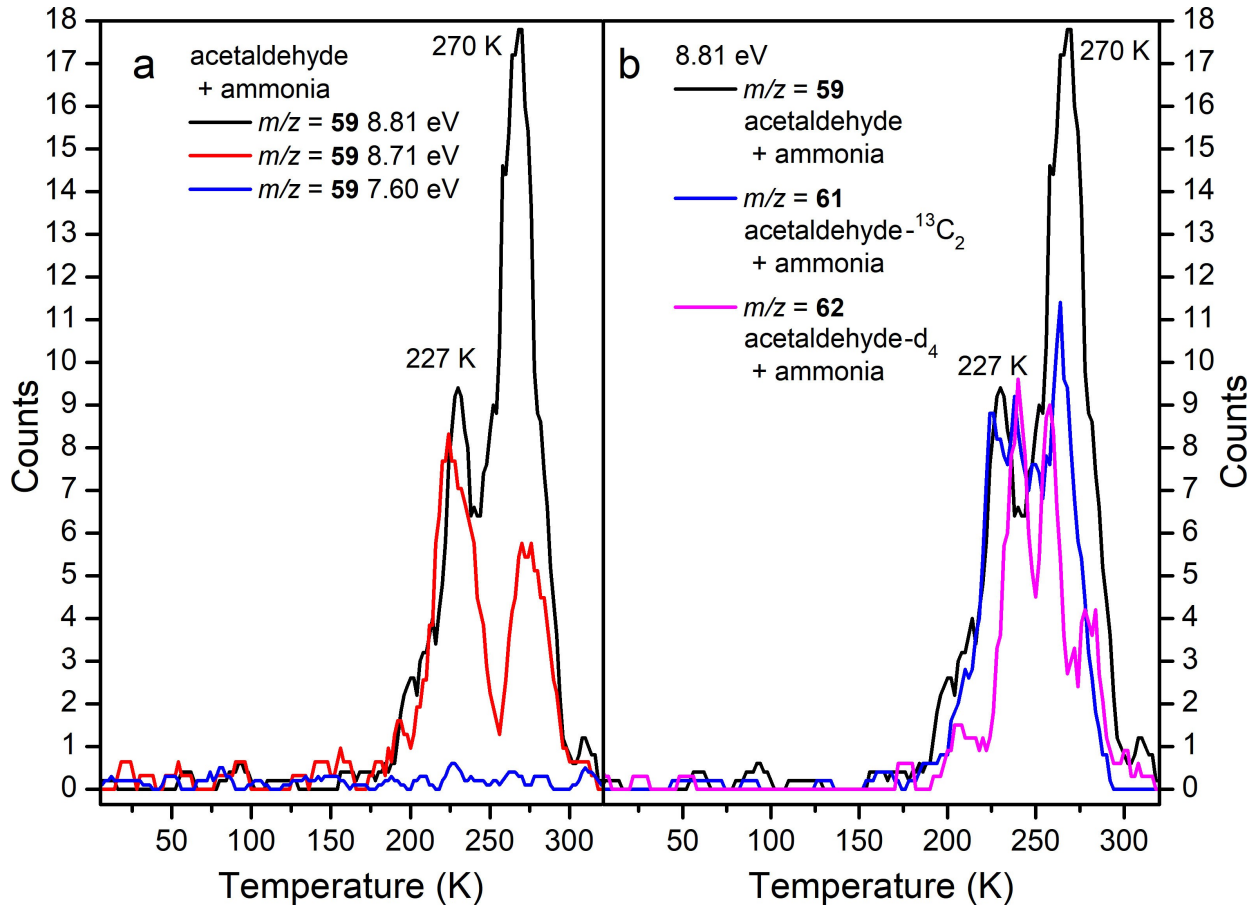

Figure 5. Ion signal during TPD of acetaldehyde and ammonia ices shown as a function of temperature. (a) Ionization of $m/z = 59$ is observed at 8.81 and 8.71 eV, but not at 7.60 eV. (b) Similar TPD profiles are observed with several isotopologues, small changes in TPD profile are observed which are likely the result of isotopic effects on rates of reaction.

photon energy. The agreement between experiment and theory here permits an unambiguous assignment of the peak observed in Figure 5 at 270 K to **6a**.

To provide further evidence on the identification of **5a**, the effects of photolysis on irradiated acetaldehyde-ammonia ices were investigated. Isomer-selective photolysis is a technique that has been used previously to both aid in the identification of the photolyzed species and to evaluate its chemical evolution during photolysis.[7c,29] The electronic absorption spectra of **5a** and **6b** were investigated with excited state calculations employing time-dependent density functional theory (TD-DFT) at the B3LYP/cc-pVTZ level (Supporting Information Figure S9 and Table S4). Isomer **5a** is predicted have the lowest energy observable transition at 185 nm and is transparent to photons with longer wavelength. However, isomer **6b** is predicted to have an absorption at 205.3 nm where **5a** is transparent, this allows **6b** to be selectively photolyzed if it is present in acetaldehyde-ammonia ices after irradiation.

Acetaldehyde-ammonia ices were subjected to photolysis both with (red curve, Figure 7) and without prior irradiation (blue curve, Figure 7) with energetic electrons (Figure 7). While PI-ReToF-MS at **8.71** eV was able to detect two similarly sized peaks assigned to **5a** and **6a** following irradiation of ices (Figure 5 and black curve in Figure 7), irradiation followed by photolysis yielded a peak for **5a** of similar intensity and a peak for **6a** with significantly increased intensity (Figure 7). This shows that **5a** is present in the ice following irradiation, if **6b** were present the peak at 227 K should have diminished or be entirely absent because of photoinitiated decomposition to ketene (H_2CCO) and ammonia or tautomerization to **2**. Of the isomers investigated computationally only **5** and **6** have ionization energies low enough to permit detection at 8.71 eV, and other isomers cannot be detected. The increase in the peak attributed to **6a** is also observed during TPD following photolysis without irradiation which must then be due to the photolytic production of **6a**. Because this is observed without irradiation it must be the result of photo-initiated reactions between ammonia and acetaldehyde. The only excited electronic state of acetaldehyde accessible with 205.3 nm photons is the lowest excited singlet state (S_1), which may undergo intersystem crossing to the lowest triplet state (T_1).[30] The S_1 and T_1 states are both the result of excitation of a non-bonding electron of oxygen into the CO anti-bonding orbital ($n \rightarrow \pi^*$).[30] This results in radical sites on the carbon and oxygen which may lead to the formation of **2** and/or **6** by photons.

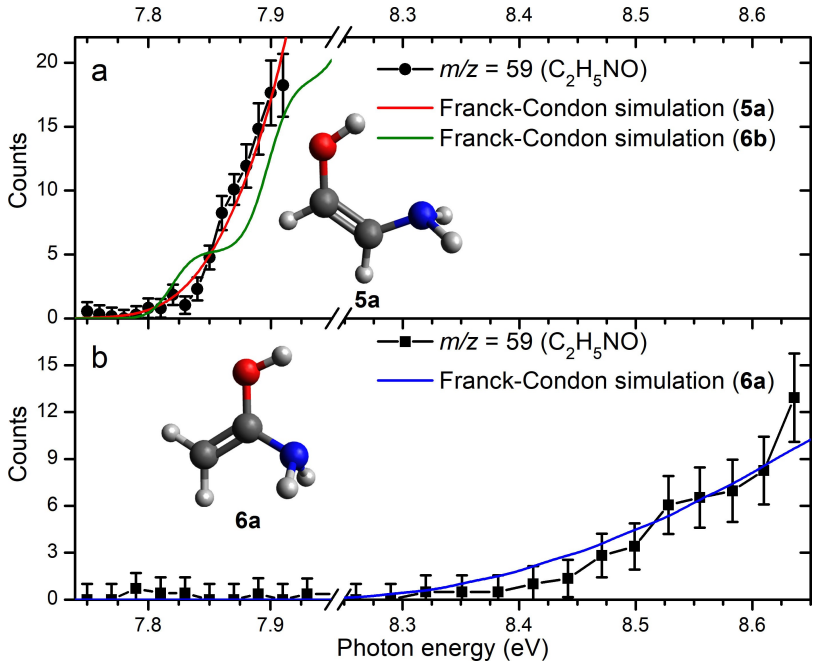

Figure 6. Photoionization efficiency (PIE) curves measured at m/z = 59 during TPD for both peaks observed in Figure 5a. Ion counts at $m/z = 59$ are plotted as a function of photon energy after correction for photon flux and temperature-dependent sublimation rate were measured from (a) 216–238 K and (b) 262–285 K. Franck–Condon simulations of the PIE curves are shown to demonstrate excellent agreement with **5a** and **6a**.

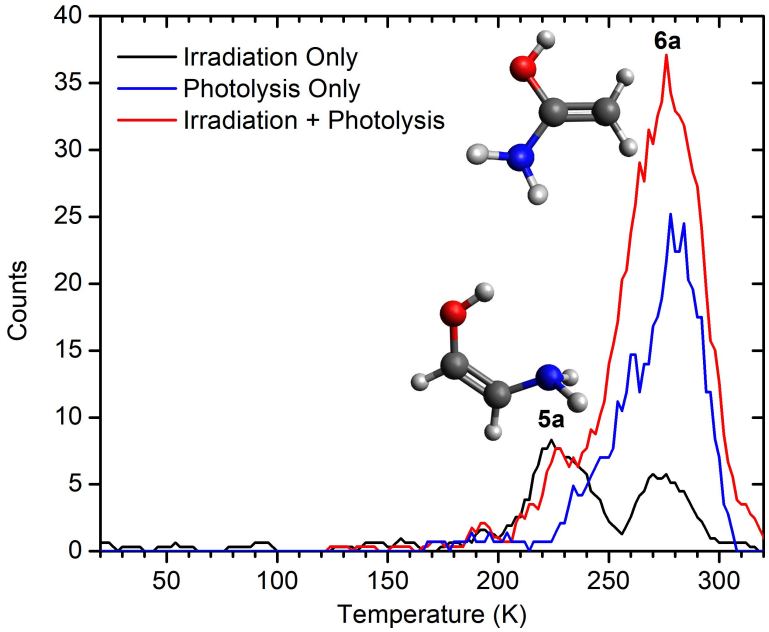

Figure 7. Signal recorded at $m/z = 59$ during TPD of acetaldehyde and ammonia ices after either irradiation or photolysis, or irradiation followed by photolysis. Ionization of the subliming neutrals was conducted with 8.71 eV photons and photolysis was conducted with 205.3 nm light. The signal attributed to **5a** is only apparent after irradiation but is unaffected by photolysis where **6b** would be photolyzed. The peak assigned to **6a** increases in intensity with photolysis, indicating a second route to its formation.

Isomers **5** and **6** reported here are isoelectronic with 1,2-ethenediol and 1,1-ethenediol (Figure 8), respectively, which have previously been observed in experiments on interstellar analog ices or in matrix isolation spectroscopic studies.[5a,27a,31] Substitution of one hydroxyl group (–OH) in 1,1-ethenediol with an amine ($–NH_2$) yields **6**. This substitution is accompanied by a significant decrease in the CCO bond angle (–8.5°), additionally the OCN bond angle is larger than the OCO bond angle (2.1°). The same substitution in 1,2-ethenediol results in several changes in

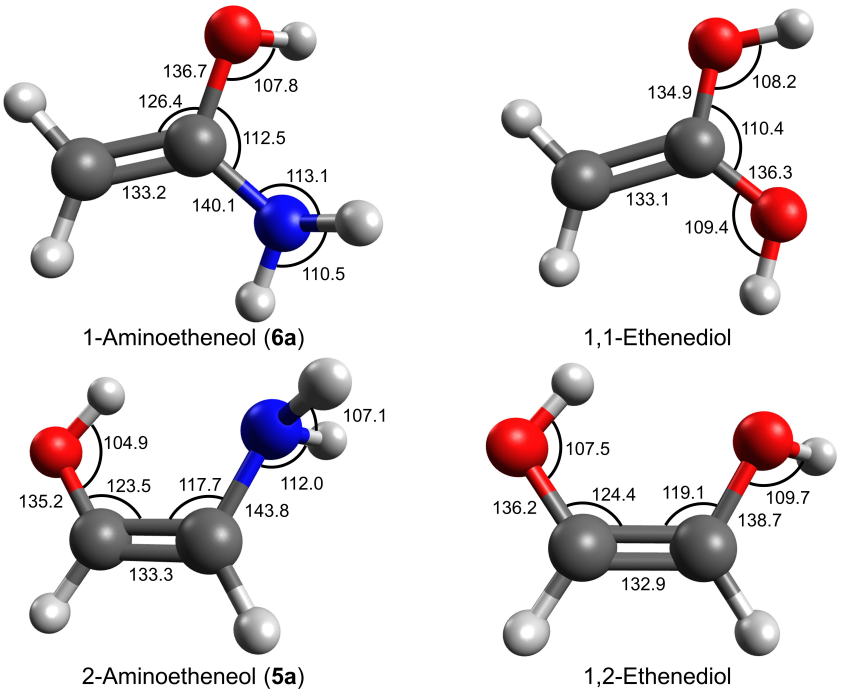

Figure 8. Structures of observed isomers of 1- and 2-aminoethenol and isoelectronic isomers of 1,1-ethenediol and 1,2-ethenediol. Structures calculated at the CCSD(T)/CBS//B3LYP/cc-pVTZ level of theory. The presented conformers of 1,1-ethenediol and 1,2-ethenediol are the most stable computed.

the geometry; *cis* and *trans* configurational isomers and conformers thereof have to be considered. Similar to the 1,1-isomer, in the *cis* isomer one of the two hydroxyl groups in 1,2-ethenediol one acts as a hydrogen-bonding donor and the other the acceptor, and it is the acceptor in the most stable conformer that is replaced with an amine in **5a**. This results in decreases in the COH bond angle (−2.6°) and CCO bond angle (−0.9°), and a CCN bond angle that is smaller (−1.4°) than the equivalent CCO bond angle. These bond angles form the perimeter of a 5-membered cyclic structure that places the hydroxyl hydrogen closest to the nitrogen non-bonding pair, and an increase in the strength of the hydrogen-bond is a likely explanation for the structural changes.

In addition to structural changes that accompany the change in substituent there are some changes that accompany the movement of the amine from one carbon to the other. The HNH bond angle is larger (3.4°) in **6a** than **5a** which can be attributed to the polarizing nature of the hydrogen bond in **5a**. Further evidence of the importance and strength of this intramolecular hydrogen bond is found in the relative energy of the different possible structures of **5** (Table S2). Internal rotation of both hydroxyl and amine bonds switches the identity of the hydrogen bond donor and acceptor, and results in a 5 kJ mol^{-1} increase in internal energy (conformer **5c**). Where **5a** has a *cis* configuration across the double bond, the two *trans* conformers are 18.6 (**5b**) and 20.4 (**5d**) kJ mol^{-1} higher in energy than **5a**. That internal rotation about the single bonds or the double bond increases energy speaks to the stabilizing effects of the 5-membered cyclic structure that permits the hydroxyl to act as the H donor and the amine to act as the acceptor.

Conclusion

The results of this study provide knowledge of how **1** and **2** along with the enol tautomers **5** and **6** can form abiotically in low temperature interstellar ices containing acetaldehyde and ammonia through processing by GCRs. The explicit detection of the **A** and **C** radicals along with the molecular structures of **1** and **2** justify barrierless radical-radical reactions with the amino radical **B** leading eventually to amides at doses readily achievable within the lifetimes of molecular clouds of a few 10^5 years (Figure 1), where the total irradiation due to GCRs is predicted to be 0.1–1 eV amu^{-1}.[18d] This irradiation dose would exceed that used in any of the experiments discussed here (Supporting Information Table S5). Utilizing IR spectroscopy along with TPD with tunable PI-ReToF-MS and PIE curves, this study identifies **1**, **2**, and their enol tautomers **5** and **6** as the dose increases from young to aged molecular clouds covering some 10^5 to 10^6 years. The non-equilibrium nature of these pathways is evident from the endoergic bond-cleavage processes forming the **A** and **C** radicals from acetaldehyde, i.e., 171 and 152 kJ mol^{-1},[32] and also from the overall endoergic pathways to **5** and **6** from **1** and **2** of 24 and 101 kJ mol^{-1}, respectively, with the energy supplied by the energetic electrons as proxies of galactic cosmic rays. This thermodynamic stability of **1** and **2** renders them relatively unreactive in comparison to their high energy tautomers **5**

and **6**—potential energy "stored" in chemical bonds through their higher enthalpies of formation that can be expended to initiate chemical reactions unavailable to their stable keto-tautomers.[7a,b,d,e]

The present experiments provide crucial first steps towards identifying formation routes to amides and amino-aldehydes, along with their high energy tautomers. This mechanistic information is accessible only using model ices comprised exclusively of the two reactants considered. In cold molecular clouds, once **1** and **2** together with **5** and **6** form within interstellar ices, the increased temperatures of the ice-coated grains upon the transition from the cold cloud to a star-forming region such as SgrB2 can lead to a sublimation of the molecules into the gas phase where they can be searched for by the Atacama Large Millimeter/submillimeter Array. Whereas **2** is "readily available" on early Earth, the limited stability of **1**, **5** and **6** has represented a tricky problem. The enol **6** has been prepared for the first time only recently as a pyrolytically generated product of a gas-phase top-down synthesis.[7c] Enol **5** has not been prepared yet and has been even suggested as "not achievable" by synthetic organic chemists.[7f] Nevertheless, the identification of the amino-enol pair **5** and **6**, which can be seen as an analogues system compared to 1,1-ethenediol ($H_2CC(OH)_2$)[27a,31] and 1,2-ethenediol (H(HO)CC-(OH)H),[5a] respectively, afford persuasive evidence that interstellar ices in cold clouds provide exotic and extreme conditions, in which enols may form.[5a,17c,33] Subsequent experiments can explore the effects of ice composition by the addition of other components common to interstellar ices such as carbon monoxide (CO), water (H_2O), methanol (CH_3OH), or investigate the effects of the composition of the grains on which ices condense by the use of silicate and carbonaceous grain analogs. However, due to the lack of high-resolution laboratory study, only two confirmed observations of enols in star-forming regions exist: vinyl alcohol (C_2H_3OH)[34] and *Z*-1,2-ethenediol (*Z*-HOCHCHOH).[5c] Once formed in molecular clouds, these complex organics can be incorporated as raw material for solar systems and into asteroids and comets.[27b,35] These reactions lead to a better understanding of the exogenous sources of prebiotic molecules on early Earth from which molecules could be assembled into peptides and proteins.

Acknowledgements

The experiments at the University of Hawaii were supported by the US National Science Foundation (NSF), Division for Astronomy (NSF-AST 2103269). The W. M. Keck Foundation and the University of Hawaii at Manoa financed the construction of the experimental setup. A.K.E. thanks the Fonds der Chemischen Industrie (Liebig Fellowship) and the Deutsche Forschungsgemeinschaft (DFG, German Research Foundation) under Germany's Excellence Strategy—EXC-2033—390677874—RESOLV for funding. Open Access funding enabled and organized by Projekt DEAL.

Conflict of Interest

The authors declare no conflict of interest.

Data Availability Statement

The data that support the findings of this study are available from the corresponding author upon reasonable request.

Keywords: Interstellar Ice · Ionization Potentials · Mass Spectrometry · Radical Reactions · Reaction Mechanism

[1] L. Mestrom, P. Bracco, U. Hanefeld, *Eur. J. Org. Chem.* **2017**, 7019–7025.
[2] E. Eichhorn, J. R. van der Ploeg, M. A. Kertesz, T. Leisinger, *J. Biol. Chem.* **1997**, *272*, 23031–23036.
[3] R. I. Kaiser, A. M. Stockton, Y. S. Kim, E. C. Jensen, R. A. Mathies, *Astrophys. J.* **2013**, *765*, 111.
[4] a) D. T. Halfen, A. J. Apponi, N. J. Woolf, R. Polt, L. M. Ziurys, *Astrophys. J.* **2006**, *639*, 237–245; b) J. M. Hollis, F. J. Lovas, P. R. Jewell, *Astrophys. J.* **2000**, *540*, L107–L110; c) J. K. Jørgensen, C. Favre, S. E. Bisschop, T. L. Bourke, E. F. van Dishoeck, M. Schmalzl, *Astrophys. J.* **2012**, *757*, L4.
[5] a) N. F. Kleimeier, A. K. Eckhardt, R. I. Kaiser, *J. Am. Chem. Soc.* **2021**, *143*, 14009–14018; b) M. Melosso, L. Bizzocchi, H. Gazzeh, F. Tonolo, J.-C. Guillemin, S. Alessandrini, V. M. Rivilla, L. Dore, V. Barone, C. Puzzarini, *Chem. Commun.* **2022**, *58*, 2750–2753; c) V. M. Rivilla, L. Colzi, I. Jiménez-Serra, J. Martín-Pintado, A. Megías, M. Melosso, L. Bizzocchi, Á. López-Gallifa, A. Martínez-Henares, S. Massalkhi, B. Tercero, P. de Vicente, J.-C. Guillemin, J. García de la Concepción, F. Rico-Villas, S. Zeng, S. Martín, M. A. Requena-Torres, F. Tonolo, S. Alessandrini, L. Dore, V. Barone, C. Puzzarini, *Astrophys. J.* **2022**, *929*, L11.
[6] a) R. Breslow, *Tetrahedron Lett.* **1959**, *1*, 22–26; b) C. Appayee, R. Breslow, *J. Am. Chem. Soc.* **2014**, *136*, 3720–3723.
[7] a) N. Heinrich, W. Koch, G. Frenking, H. Schwarz, *J. Am. Chem. Soc.* **1986**, *108*, 593–600; b) J.-F. Lin, C.-C. Wu, M.-H. Lien, *J. Phys. Chem.* **1995**, *99*, 16903–16908; c) A. Mardyukov, F. Keul, P. R. Schreiner, *Chem. Sci.* **2020**, *11*, 12358–12363; d) J. P. Richard, G. Williams, A. C. O'Donoghu, T. L. Amyes, *J. Am. Chem. Soc.* **2002**, *124*, 2957–2968; e) D. Schröder, J. Loos, R. Thissen, O. Dutuit, P. Mourgues, H.-E. Audier, C. Lifshitz, H. Schwarz, *Angew. Chem. Int. Ed.* **2002**, *41*, 2748–2751; *Angew. Chem.* **2002**, *114*, 2867–2870; f) K. M. Reddy, B. Thirupathi, E. J. Corey, *Org. Lett.* **2017**, *19*, 4956–4959.
[8] a) M. J. Nowak, L. Lapinski, J. Fulara, *Spectrochim. Acta Part A* **1989**, *45*, 229–242; b) M. K. Shukla, J. Leszczynski, *WIREs Comput. Mol. Sci.* **2013**, *3*, 637–649.
[9] N. Kitadai, S. Maruyama, *Geosci. Front.* **2018**, *9*, 1117–1153.
[10] a) W. Martin, M. J. Russell, *Philos. Trans. R. Soc. London Ser. B* **2007**, *362*, 1887–1925; b) K. H. Lemke, R. J. Rosenbauer, D. K. Bird, *Astrobiology* **2009**, *9*, 141–146.
[11] J. L. Bada, *Chem. Soc. Rev.* **2013**, *42*, 2186–2196.
[12] D. T. Halfen, V. Ilyushin, L. M. Ziurys, *Astrophys. J.* **2011**, *743*, 60.
[13] a) K. Altwegg, H. Balsiger, J. J. Berthelier, A. Bieler, U. Calmonte, S. A. Fuselier, F. Goesmann, S. Gasc, T. I. Gombosi, L. Le Roy, J. de Keyser, A. Morse, M. Rubin, M. Schuhmann, M. G. G. T. Taylor, C. Y. Tzou, I. Wright, *Mon. Not. R. Astron. Soc.* **2017**, *469*, S130–S141; b) J. M. Hollis, F. J. Lovas, A. J. Remijan, P. R. Jewell, V. V. Ilyushin, I. Kleiner, *Astrophys. J.* **2006**, *643*, L25–L28.

[14] a) A. Belloche, A. A. Meshcheryakov, R. T. Garrod, V. V. Ilyushin, E. A. Alekseev, R. A. Motiyenko, L. Margulès, H. S. P. Müller, K. M. Menten, *Astron. Astrophys.* **2017**, *601*, A49; b) L. Foo, A. Surányi, A. Guljas, M. Szőri, J. J. Villar, B. Viskolcz, I. G. Csizmadia, A. Rágyanszki, B. Fiser, *Mol. Astrophys.* **2018**, *13*, 1–5.
[15] a) A. J. Remijan, L. E. Snyder, B. A. McGuire, H.-L. Kuo, L. W. Looney, D. N. Friedel, G. Y. Golubiatnikov, F. J. Lovas, V. V. Ilyushin, E. A. Alekseev, S. F. Dyubko, B. J. McCall, J. M. Hollis, *Astrophys. J.* **2014**, *783*, 77; b) A. Belloche, R. T. Garrod, H. S. P. Müller, K. M. Menten, I. Medvedev, J. Thomas, Z. Kisiel, *Astron. Astrophys.* **2019**, *628*, A10.
[16] J. Li, J. Wang, X. Lu, V. Ilyushin, R. A. Motiyenko, Q. Gou, E. A. Alekseev, D. Quan, L. Margulès, F. Gao, F. J. Lovas, Y. Wu, E. Bergin, S. Li, Z. Shen, F. Du, M. Li, S. Zheng, X. Zheng, *Astrophys. J.* **2021**, *919*, 4.
[17] a) R. E. Johnson, *Energetic Charged-Particle Interactions with Atmospheres and Surfaces*, Springer, Berlin, Heidelberg, **1990**; b) C. J. Bennett, C. S. Jamieson, Y. Osamura, R. I. Kaiser, *Astrophys. J.* **2005**, *624*, 1097–1115; c) C. J. Bennett, Y. Osamura, M. D. Lebar, R. I. Kaiser, *Astrophys. J.* **2005**, *634*, 698–711.
[18] a) R. T. Garrod, S. L. W. Weaver, E. Herbst, *Astrophys. J.* **2008**, *682*, 283–302; b) R. T. Garrod, *Astrophys. J.* **2013**, *765*, 60; c) H. M. Cuppen, C. Walsh, T. Lamberts, D. Semenov, R. T. Garrod, E. M. Penteado, S. Ioppolo, *Space Sci. Rev.* **2017**, *212*, 1–58; d) A. G. Yeghikyan, *Astrophys. J.* **2011**, *54*, 87–99.
[19] J. B. Pollack, D. Hollenbach, S. Beckwith, D. P. Simonelli, T. Roush, W. Fong, *Astrophys. J.* **1994**, *421*, 615–639.
[20] a) E. L. Gibb, D. C. B. Whittet, A. C. A. Boogert, A. G. G. M. Tielens, *Astrophys. J. Suppl. Ser.* **2004**, *151*, 35–73; b) C. R. Arumainayagam, R. T. Garrod, M. C. Boyer, A. K. Hay, S. T. Bao, J. S. Campbell, J. Wang, C. M. Nowak, M. R. Arumainayagam, P. J. Hodge, *Chem. Soc. Rev.* **2019**, *48*, 2293–2314.
[21] P. D. Holtom, C. J. Bennett, Y. Osamura, N. J. Mason, R. I. Kaiser, *Astrophys. J.* **2005**, *626*, 940–952.
[22] S. Bottinelli, A. C. A. Boogert, J. Bouwman, M. Beckwith, E. F. van Dishoeck, K. I. Öberg, K. M. Pontoppidan, H. Linnartz, G. A. Blake, N. J. Evans, F. Lahuis, *Astrophys. J.* **2010**, *718*, 1100–1117.
[23] B. M. Jones, R. I. Kaiser, *J. Phys. Chem. Lett.* **2013**, *4*, 1965–1971.
[24] a) A. M. Turner, R. I. Kaiser, *Acc. Chem. Res.* **2020**, *53*, 2791–2805; b) M. J. Abplanalp, M. Förstel, R. I. Kaiser, *Chem. Phys. Lett.* **2016**, *644*, 79–98.
[25] O. Kostko, B. Bandyopadhyay, M. Ahmed, *Annu. Rev. Phys. Chem.* **2016**, *67*, 19–40.
[26] A. Bergantini, M. J. Abplanalp, P. Pokhilko, A. I. Krylov, C. N. Shingledecker, E. Herbst, R. I. Kaiser, *Astrophys. J.* **2018**, *860*, 108.
[27] a) N. F. Kleimeier, R. I. Kaiser, *J. Phys. Chem. Lett.* **2022**, *13*, 229–235; b) N. F. Kleimeier, A. K. Eckhardt, P. R. Schreiner, R. I. Kaiser, *Chem* **2020**, *6*, 3385–3395; c) J. Wang, J. H. Marks, A. M. Turner, A. A. Nikolayev, V. Azyazov, A. M. Mebel, R. I. Kaiser, *Phys. Chem. Chem. Phys.* **2023**, *25*, 936–953.
[28] J. M. Hollas, *Modern Spectroscopy* > 4th ed., Wiley, Chichester, **2004**.
[29] a) J. Xu, Z. Wu, H. Wan, G. Deng, B. Lu, A. K. Eckhardt, P. R. Schreiner, T. Trabelsi, J. S. Francisco, X. Zeng, *J. Am. Chem. Soc.* **2018**, *140*, 9972–9978; b) H. P. Reisenauer, G. Mloston, J. Romanski, P. R. Schreiner, *Eur. J. Org. Chem.* **2011**, 6269–6275; c) C. Zhu, A. K. Eckhardt, S. Chandra, A. M. Turner, P. R. Schreiner, R. I. Kaiser, *Nat. Commun.* **2021**, *12*, 5467; d) C. Zhu, A. K. Eckhardt, A. Bergantini, S. K. Singh, P. R. Schreiner, R. I. Kaiser, *Sci. Adv.* **2020**, *6*, eaba6934.
[30] P. Limão-Vieira, S. Eden, N. J. Mason, S. V. Hoffmann, *Chem. Phys. Lett.* **2003**, *376*, 737–747.
[31] A. Mardyukov, A. K. Eckhardt, P. R. Schreiner, *Angew. Chem. Int. Ed.* **2020**, *59*, 5577–5580; *Angew. Chem.* **2020**, *132*, 5625–5628.
[32] B. Ruscic, D. H. Bross, "Active Thermochemical Tables (ATcT) values based on ver. 1.122r of the Thermochemical Network", can be found under http://atct.anl.gov, **2021**.
[33] N. F. Kleimeier, R. I. Kaiser, *ChemPhysChem* **2021**, *22*, 1229–1236.
[34] B. E. Turner, A. J. Apponi, *Astrophys. J.* **2001**, *561*, L207–L210.
[35] a) J. R. Cronin, C. B. Moore, *Science* **1971**, *172*, 1327–1329; b) G. Cooper, C. Reed, D. Nguyen, M. Carter, Y. Wang, *Proc. Natl. Acad. Sci. USA* **2011**, *108*, 14015–14020.

Manuscript received: December 16, 2022
Accepted manuscript online: January 26, 2023
Version of record online: ■■, ■■

Research Articles

Reaction Mechanisms

J. H. Marks, J. Wang, N. F. Kleimeier, A. M. Turner, A. K. Eckhardt,* R. I. Kaiser* _____ e202218645

Prebiotic Synthesis and Isomerization in Interstellar Analog Ice: Glycinal, Acetamide, and Their Enol Tautomers

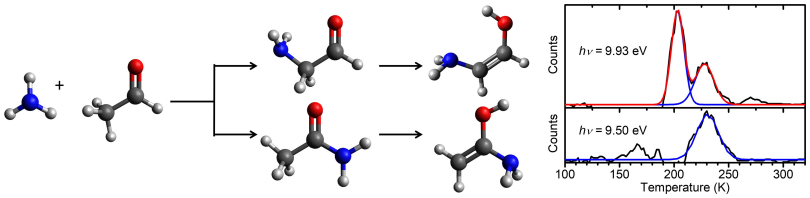

Out of the cold: Ammonia (NH_3) and acetaldehyde (CH_3CHO) are exposed to galactic cosmic ray proxies while frozen at 5 K to simulate the environment of an interstellar molecular cloud. Reactants undergo dissociation and radical recombination to produce glycinal (NH_2CH_2CHO) and acetamide (CH_3CONH_2) prior to tautomerization to 2-aminoethenol ($HOCHCHNH_2$) and 1-aminoethenol ($H_2CC(OH)NH_2$), respectively.